Separation Science and Technology
Publication details, including instructions for authors and subscription information:
http://www.informaworld.com/smpp/title~content=t713708471

Batch Adsorber Rate Analysis of Methylene Blue on Amberlite and Clinoptilolite

Julide Yener[a]; Turkan Kopac[a]; Gulsen Dogu[b]; Timur Dogu[c]
[a] Department of Chemistry, Zonguldak Karaelmas University, Zonguldak, Turkey [b] Department of Chemical Engineering, Gazi University, Ankara, Turkey [c] Department of Chemical Engineering, Middle East Technical University, Ankara, Turkey

To cite this Article Yener, Julide , Kopac, Turkan , Dogu, Gulsen and Dogu, Timur(2006) 'Batch Adsorber Rate Analysis of Methylene Blue on Amberlite and Clinoptilolite', Separation Science and Technology, 41: 9, 1857 — 1879
To link to this Article: DOI: 10.1080/01496390600674851
URL: http://dx.doi.org/10.1080/01496390600674851

Separation Science and Technology, 41: 1857–1879, 2006

ISSN 0149-6395 print/1520-5754 online
DOI: 10.1080/01496390600674851

Batch Adsorber Rate Analysis of Methylene Blue on Amberlite and Clinoptilolite

Julide Yener and Turkan Kopac
Department of Chemistry, Zonguldak Karaelmas University, Zonguldak, Turkey

Gulsen Dogu
Department of Chemical Engineering, Gazi University, Ankara, Turkey

Timur Dogu
Department of Chemical Engineering, Middle East Technical University, Ankara, Turkey

Abstract: Adsorption of Methylene Blue on clinoptilolite and on Amberlite XAD-4 was investigated in a temperature range of 20–50°C, in a batch adsorber. Results of this work showed that clinoptilolite was a better sorbent than Amberlite XAD-4 for the removal of Methylene Blue. Among the four adsorption rate models tested in the analysis of the adsorption rate data, a simple single parameter diffusion model (Model C) was shown as the best model to be used in practical applications. The diffusivity found from this model was not dependent on the adsorbate concentration. Although the pseudo-first order adsorption rate model also gave good agreement with the experimental data obtained at the initial periods of the adsorption experiments, the concentration dependence of the rate constant of this model was found as the major disadvantage of this model. Results indicated that dissociative chemisorption and blocking of some of the pores during adsorption caused high tortuosity factors and a decrease in the adsorption rate. Adsorption capacity of these adsorbents were also found to be increased significantly by a decrease of the pH of the solution from 10 to 3.

Keywords: Clinoptilolite, Amberlite XAD-4, Methylene Blue, adsorption, effective diffusivity, moment technique

Received 17 August 2005, Accepted 20 February 2006
Address correspondence to Turkan Kopac, Department of Chemistry, Zonguldak Karaelmas University, 67100, Zonguldak, Turkey. E-mail: turkankopac@yahoo.com

INTRODUCTION

Removal of dyes and pigments from the waste water streams discharged from textile and paint industries is an important environmental issue. Due to the biological and chemical stabilty of most of the dyes, adsorption is considered as an attractive alternate (1–6) for the removal of dyes and the other chemicals from the waste water streams. Adsorption of organic molecules from aqueous solutions on various adsorbents have been investigated by number of researchers. McKay et al. (1, 2) investigated the adsorption of acidic, basic, disperse, and direct dyes from aqueous solutions on activated carbon. In another study (3), adsorption of a basic dye (Astrozone Blue-Basic Blue 69) and an acidic dye (Teflon Blue) on Fuller's earth and on fired clay were investigated. Adsorption capacities of number of natural adsorbents, such as wood, rice husk, coal, teakwood bark, cotton waste, sawdust, bagasse pith (waste product from sugar industry) and different types of clays such as bentonite, kaolinite etc. for the removal of different dyes were investigated by a number of researchers (4–13). Khare et al. (14) investigated the removal of Victoria Blue from aqueous solutions by fly ash. Gupta et al. (15) used fly ash and coal combinations as mixed adsorbents for the removal of omega chrome dye. Significance of surface modification of silicas on the adsorption of dyes was investigated by Khokhlova et al. (12). It was also shown in the literature that (16), chrome sludge, which is the waste product of electroplating industries, may also be used for color removal from the waste water streams. Adsorption of Basic Yellow 28 on clinoptilolite (a natural zeolite) and on an acidic resin (Amberlite) was investigated in our recent study (17). In that work, both adsorption rate data of Basic Yellow 28 and the adsorption capacities of these sorbents were reported. Adsorption capacities of some biosorbents for colour removal were also investigated in the literature. In the study of Wang and Yu (18), adsorption of different dyes on biosorbents, such as living mycelium of white rot fungus, was investigated and the maximum adsorption capacities were reported. In the recent publication of Rubin et al. (19), experimental results were reported for the adsorption of Methylene Blue on Sargassum muticum, which is an invasive macroalga and it was claimed that this low cost biosorbent could be successfully used in waste water treatment.

Detailed information about the adsorption rate as well as the adsorption capacity of an adsorbate are needed for the design of adsorption equipment. Adsorption rate data obtained from the experimental concentration decay curves of an adsorbate in a liquid phase batch adsorber may be analyzed by using number of different adsorption rate models. The conventional pseudo-first order (15) and the pseudo-second order (18) adsorption rate models do not consider the effects of pore diffusion resistances on the adsorption rates. However, diffusional effects may be quite important in a number of adsorption processes. In the case of significant diffusional effects, the observed rate constants evaluated from the first and the second order

adsorption rate models are expected to be significantly dependent on the pore diffusion rate. Another approach for the description of the adsorption rate of an adsorbate on a porous adsorbent is the use of diffusion models proposed for such systems (20).

In the present study, adsorption rate and equilibrium of Methylene Blue is investigated in a batch adsorber, using clinoptilolite (a natural zeolite) and Amberlite XAD-4 as the adsorbents. Significance of pore diffusion resistance on the adsorption rate is also investigated. Adsorption rate data are analyzed by using different models and the results are compared. Also, the adsorption equilibrium data obtained for these systems are analyzed using Langmuir and Freundlich adsorption isotherms.

ADSORPTION RATE MODELS

For a pseudo-first order reversible adsorption process, the species conservation equation of an adsorbate in the liquid phase of a batch adsorber can be expressed in terms of the rate of adsorption R_A ((mg adsorbed)/s·(g adsorbent)) as,

$$\left(\frac{1}{w_s}\right)\frac{dC}{dt} = R_A = -(k_1^* C(q_m - q) - k_{-1}^* q) = -\frac{dq}{dt} \tag{1}$$

Here, q_m and w_s are the maximum possible adsorbed concentration (mg/g adsorbent) corresponding to the complete coverage of all the available sites of adsorbent by the adsorbate molecules and the amount of adsorbent per unit liquid volume (g/l) in the adsorber, respectively. Integration of equation (1) with ($C_o = qw_s + C$) gives a relation between adsorbed concentration q and time.

$$\ln\left[\left(\frac{q_e - q}{q_e}\right)\left(\frac{C_o q_m/q_e}{(C_o q_m/q_e) - qw_s}\right)\right] = -k_1^*((C_o q_m/q_e) - q_e w_s)t \tag{2}$$

For small values of q, $\left(q < \left(C_o q_m / q_e w_s\right)\right)$, which correspond to the early times of an adsorption run carried out in the batch adsorber, equation (2) can be simplified as,

$$\ln(q_e - q) = \ln q_e - k_1 t \quad \text{(Model A)} \tag{3}$$

This is the well–known Lagergren equation used in the predictions of adsorption rate in batch adsorbers (15). In equation (3), the observed rate constant $k_1 = k_1^*\left(\left(C_o q_m/q_e\right) - q_e w_s\right)$ depends upon the initial adsorbate concentration in the liquid, as well as the mass of the adsorbent charged to the adsorber per unit liquid volume (w_s) and the adsorbed concentration of the adsorbate at equilibrium (q_e). Also, this model does not consider diffusional effects on the observed rate. In the case of significant pore diffusion effects, observed adsorption rate constant is also expected to be dependent on the effective

pore diffusivity and the particle size of the adsorbent. This model (Model A) may be used for the evaluation of observed adsorption rate constant in dilute systems or at the early times of the batch adsorber adsorption experiments.

A pseudo-second order adsorption rate model was also used in some studies. According to this second order model, the relation between the adsorbed concentration q and time was proposed as (18),

$$\frac{1}{(q_e - q)} = \frac{1}{q_e} + k_2 t \quad \text{(Model B)} \tag{4}$$

The limitations of this model are similar to the limitations of Model A. The observed second order rate constant k_2 is also expected to be dependent on the pore diffusion parameters, initial adsorbate concentration and the amount of adsorbent charged to the adsorber.

Pore diffusion resistance may be the rate controlling step in many of the adsorption processes. In such a case, the species conservation equation for the adsorbate in the liquid phase of the batch adsorber may be written by equating the depletion rate of the adsorbate to its rate of transport into the porous adsorbent particles (20). The rate of transport of the adsorbate into the porous adsorbent particles is expressed as the product of diffusion flux at the external surface of the particles (at $R = R_o$) with the external surface area of the paricles. For this case, species conservation equation for the adsorbate in the liquid phase of the batch adsorber may be expressed as,

$$\frac{dC}{dt} = -\left(\frac{w_s}{\rho_p}\right)\left(\frac{3}{R_o}\right) D_A \left[\frac{\partial C_A}{\partial R}\right]_{R=R_o} \tag{5}$$

The evaluation of the adsorption rate from this model requires information about the concentration profile within the porous adsorbent. The pseudo-homogeneous species conservation equation in the pores of a spherical adsorbent having an average particle radius of R_o, may be written as,

$$\frac{D_A}{R^2}\frac{\partial}{\partial R}\left(R^2 \frac{\partial C_A}{\partial R}\right) = \frac{\partial C_A}{\partial t} \quad \text{(Model C)} \tag{6}$$

Using the symmetry boundary condition at $R = 0$ and by taking $C_A = C$ at $R = R_o$, the model equations may be solved.

The moment technique was frequently used in the literature in the evaluation of adsorption, diffusion, and reaction rate parameters within porous solids and in fixed bed adsorbers (21–24). In the early work of Furusawa and Suzuki (23), application of the moment technique to batch adsorbers was proposed. This technique was further extended in our recent work (20) for the evaluation of diffusion resistances and the surface diffusion parameters in porous solids placed in a batch adsorber. For a batch adsorber, the zeroth moment (μ_0) corresponds to the area under the decay curve of the dimensionless

adsorbate concentration, and it is defined as:

$$\mu_o = \int_0^\infty \frac{(C - C_e)}{(C_o - C_e)} dt \tag{7}$$

In the moment technique, the species conservation equation (Equation (6)) describing the dynamic system under investigation was solved in Laplace domain and the moment expressions were then derived (20, 23) using,

$$\mu_n = (-1)^n \lim_{s \to 0} \frac{d^n}{ds^n} \left(\frac{(\overline{C - C_e})}{(C_o - C_e)} \right); \quad n = 0, 1, 2, 3 \text{ etc.} \tag{8}$$

Here, s and $(\overline{C - C_e})$ correspond to the Laplace variable and Laplacian of $(C - C_e)$, respectively. Following this procedure, the zeroth moment expression for the concentration decay curve was then derived for this model as,

$$\mu_o = \frac{R_o^2}{15 D_A \left(1 + \dfrac{w_s}{\rho_p} \right)} \quad \text{(Model C)} \tag{9}$$

Experimental μ_o values may be evaluated by the numerical integration of equation (7) using the concentration decay data of the adsorbate, obtained in a batch adsorber. These experimental zeroth moment values may then be used for the evaluation of effective diffusion coefficient D_A from equation (9). The only unknown of this single parameter model (Model C) is the effective diffusion coefficient. In this model, adsorption of the adsorbate is not considered as a separate term. The effective diffusivity of this model also includes such adsorption effects.

In another model proposed in the recent publication of Dogu et al. (20), adsorption and the pore diffusion terms were separately included into the species conservation equation. For this model (Model D), equation (6) should be replaced by equation (10).

$$\frac{D_A}{R^2} \frac{\partial}{\partial R} \left(R^2 \frac{\partial C_A}{\partial R} \right) = (\varepsilon_A + \rho_p K) \frac{\partial C_A}{\partial t} \tag{10}$$

For this model, the zeroth moment expression is given by Dogu et al. (20),

$$\mu_o = \frac{R_o^2 (\varepsilon_A + \rho_p K)}{15 D_A \left(1 + \dfrac{w_s}{\rho_p} (\varepsilon_A + \rho_p K) \right)} \quad \text{(Model D)} \tag{11}$$

In the derivation of this model, a linear adsorption relation was assumed between q and C_A. It was shown by Dogu et al. (20) that the observed adsorption equilibrium constant K which appear in equation (11) may be estimated from the slope of the adsorption isotherm at C_e. For Freundlich and

Langmuir type adsorption isotherms, K may be estimated from the slopes of the isotherms (20) using the following expressions.

$$\text{Freundlich Isotherm: } q = K_f C_e^n; \quad K = nK_f C_e^{n-1} \tag{12}$$

$$\text{Langmuir Isotherm: } \frac{q}{q_m} = \frac{K_A C_e}{1 + K_A C_e}; \quad K = \frac{q_m K_A}{(1 + K_A C_e)^2} \tag{13}$$

In the present study, all four of these models were used for the estimation of adsorption rate parameters of Methylene Blue on clinoptilolite and Amberlite XAD-4 and the results were compared.

EXPERIMENTAL WORK

In this study, natural clinoptitolite from the Bigadic region of Turkey and Amberlite XAD-4 were used as the adsorbents for the removal of Methylene Blue from solutions. Methylene Blue is a monovalent cationic dye. Some physical properties of Methylene Blue are reported in Table 1 (25). Clinoptitolite is a natural zeolite and Amberlite XAD-4 is a porous polymeric resin. Their pore size distributions, apparent and solid densities and the surface areas were determined using mercury porosimeter (Micrometrics 9310), helium pycnometer and single point nitrogen adsorption surface area analyzer (Quantachrome) equipment. Some physical properties of these adsorbents are given in Table 2. The surface area values reported in that table correspond to the macro and the meso-pores. The clinoptitolite samples were first sieved, particles having an average diameter of 0.015 cm were dried at 100°C under vacuum for 24 hours and stored under vacuum before using in the adsorption experiments.

Adsorption rate experiments were carried out in a 3000 ml batch adsorber. In most experiments, 2750 ml of dye solution, with an initial concentration of 13 mg/l, was charged to the adsorber, which was mixed at a rate of 120 rpm using a magnetic stirrer. Adsorption rate experiments were started by charging predetermined amounts of adsorbent into the adsorber. Experiments were carried out at different temperatures in a range between 20–50°C. In another set of experiments, the effect of pH was investigated at constant temperature. At predetermined time intervals, 3 ml samples were taken out of the

Table 1. Some physical properties of Methylene Blue (25)

Chemical formula	$C_{16}H_{18}ClN_3S \cdot xH_2O$ ($x = 2$–3)
Bulk density	400–600 kg/m^3
Solubility in water	50 g/l (at 20°C)
Odour and form	Odourless and dark blue

Table 2. Physical properties of the adsorbents

Adsorbent	Clinoptilolite	Amberlite XAD-4
Particle radius (cm)	0.0075	0.021
Total porosity	0.53	0.52
Apparent density (g/cm^3)	0.76	0.56
Surface area (m^2/g)	37	750

adsorber and immediately analyzed spectrophotometrically (Pharmacia LKB-Novaspec II) at a wavelength of 665 nm.

The adsorption equilibrium isotherms were determined at different temperatures using a bottle-point procedure. Different amounts of adsorbents were put into each of six to ten bottles. The bottles were then filled with Methylene Blue solution and were left to shake in a constant temperature bath. Upon equilibriation, samples taken from each bottle were again analyzed spectrophotometrically.

RESULTS AND DISCUSSIONS

Comparison of the Adsorption Rates with Clinoptilolite and Amberlite XAD-4

Typical adsorption rate data obtained at 20°C for the adsorption of Methylene Blue using different amounts of clinoptilolite and Amberlite XAD-4 adsorbents are reported in Figs. 1 and 2, respectively. Comparison of the data presented in these two figures showed that adsorption rate values obtained with clinoptilolite were higher than the corresponding values obtained with Amberlite XAD-4. As it is shown in Fig. 1, concentration of Methylene Blue reached the equilibrium value within about 1000 min, especially for amounts of clinoptitolite higher than 1.14 g/l charged to the adsorber. Much longer times were needed to reach equilibrium with Amberlite XAD-4 (Fig. 2). The data reported in these figures were then used for the prediction of the rate constants of the pseudo-first order and the second order adsorption rate models. In these analysis, data obtained at early times of the adsorption process were used. Typical Lagergren plots (Model A) corresponding to the pseudo-first order adsorption rate model (Equation (3)) obtained with clinoptilolite and Amberlite XAD-4 are given in Figs. 3 and 4, respectively. Similarly, some typical plots corresponding to the pseudo-second order model (Model B) are shown in Figs. 5 and 6, for clinoptilolite and Amberlite XAD-4, respectively. Data fit to the linear relation obtained in Model A (Equation (3)) was more satisfactory (r^2 values of linear regression were in the range of 0.93–0.99) than the corresponding fit to the second order model (Model B, Equation (4)). For the second case, r^2 values were around 0.87–0.97. From these results it was concluded that, among the

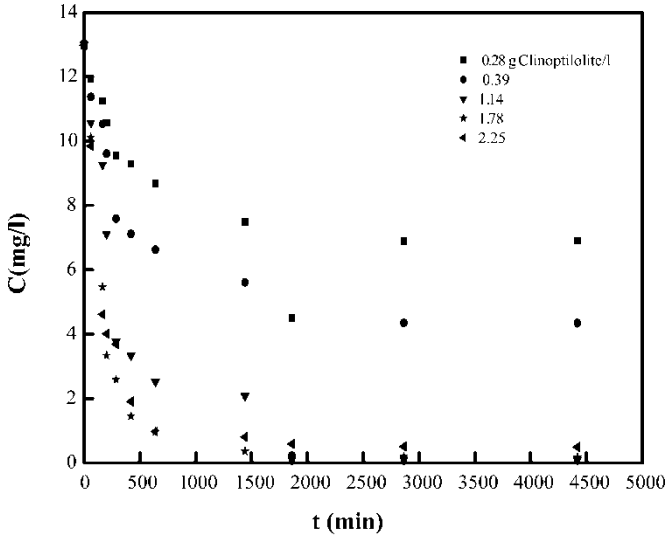

Figure 1. Batch adsorber data for Methylene Blue adsorption on clinoptilolite ($T = 20^{\circ}C$).

first order and the second order models, Model A (first order model) is a better representation of adsorption rate.

Observed pseudo-first order adsorption rate constant values of Methylene Blue on clinoptilolite and Amberlite XAD-4 were evaluated from the slopes

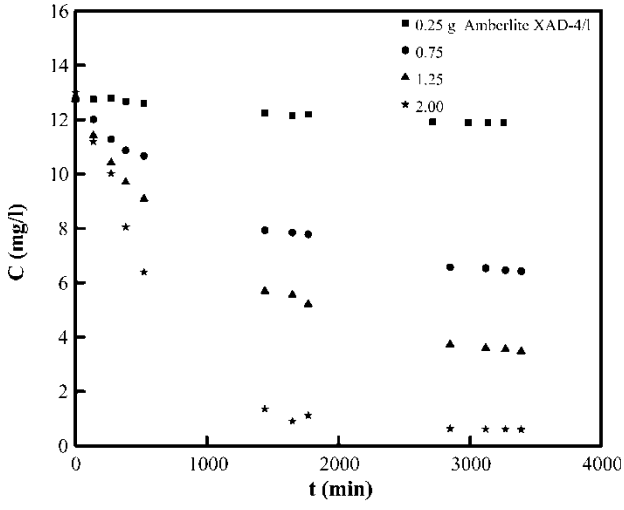

Figure 2. Batch adsorber data for Methylene Blue adsorption on Amberlite XAD-4 (T= 20°C).

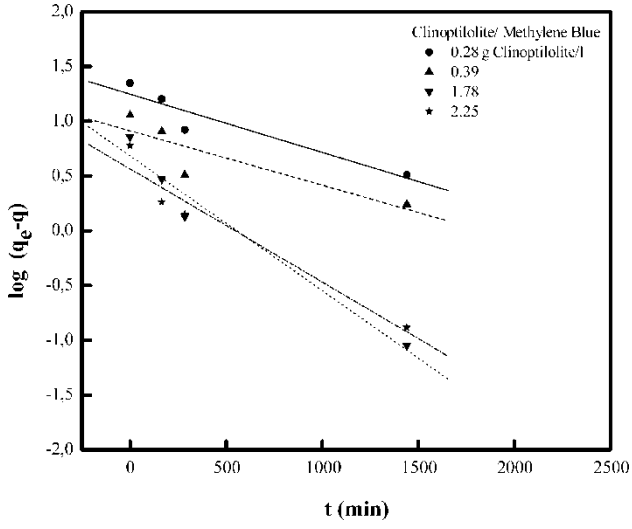

Figure 3. Typical Lagergren plots for adsorption of Methylene Blue on clinoptilolite at 20°C.

of the linear Lagergren plots (Figs. 3 and 4). Typical pseudo-first order rate constant values are reported in Table 3. In the same table, pseudo-second order rate constants evaluated from the slopes of plots given in Figs. 5 and 6 are also reported. As is seen in Table 3, the first order adsorption rate

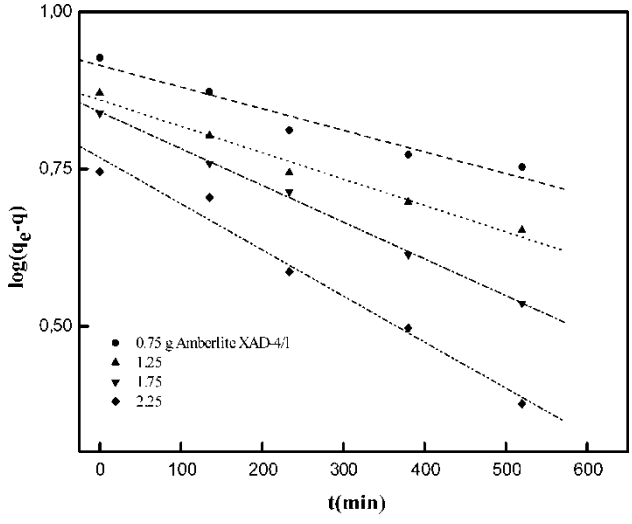

Figure 4. Typical Lagergren plots for adsorption of Methylene Blue on Amberlite XAD-4 at 20°C.

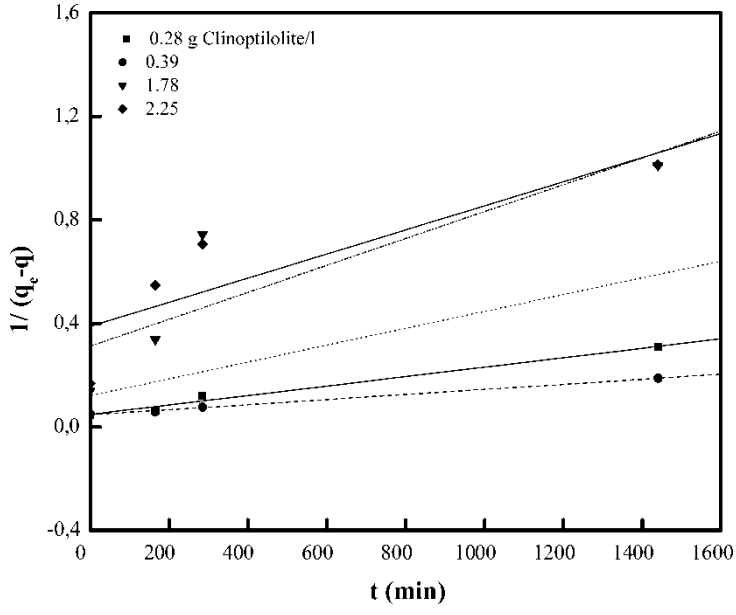

Figure 5. Typical second order plots for adsorption of Methylene Blue on clinoptilolite at 20°C.

constants (k_1) obtained with clinoptilolite were greater than the corresponding values obtained with Amberlite XAD-4. For both sorbents, k_1 values were found to increase with an increase in the amount of adsorbent charged to the adsorber. As it is discussed above in the model development section, the observed pseudo-first order and the pseudo-second order rate constants are expected to be dependent upon the amount of adsorbent as well as the initial and the equilibrium concentrations of the adsorbate. The concentration dependence of the rate constants of the pseudo-first order and the second order adsorption rate models limits the general application of these models in the prediction of the adsorption rates of Methylene Blue on clinoptilolite and Amberlite XAD-4.

Using the data obtained at very long times of contact, equilibrium values of the fluid phase concentration and the corresponding values of the adsorbed concentration of the dye were also determined. These data were used to construct the adsorption isotherms. The data obtained for the adsorption of Methylene Blue on clinoptilolite and Amberlite XAD-4 at 20°C are fitted to the Langmuir and the Freundlich adsorption isotherms and the results are summarized in Table 4. Langmuir isotherm gave a better fit to the adsorption equilibrium data. As seen in this table, the maximum possible adsorption capacity of clinoptitolite, corresponding to the monolayer coverage of all the sites by the adsorbate (q_m value of the Langmuir adsorption isotherm), is much higher than the corresponding value obtained with Amberlite XAD-4, indicating a

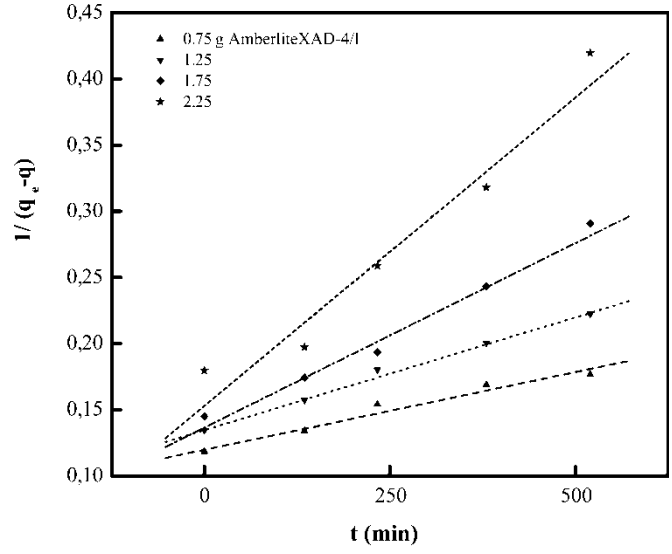

Figure 6. Typical second order plots for adsorption of Methylene Blue on Amberlite XAD-4 at 20°C.

higher adsorption capacity of this sorbent. As it was discussed above, adsorption rate values obtained with this adsorbent were also higher than the corresponding values obtained with Amberlite XAD-4. Both adsorption equilibrium and the adsorption rate results showed that clinoptilolite was a better adsorbent for

Table 3. Adsorption rate constants of Methylene Blue on clinoptilolite and on Amberlite XAD-4 for the pseudo-first order (Model A-Equation (3)) and the second order (Model B-Equation (4)) models. ($T = 20°C$; $C_o = 13$ mg/l)

Amount of adsorbent (g/l)	k_1 (min^{-1})	k_2 (g/mg · min)
Clinoptilolite		
0.28	0.0012	0.00018
0.39	0.0015	0.00010
1.78	0.0028	0.00053
2.25	0.0024	0.00047
Amberlite XAD-4		
0.25	0.00039	0.00012
0.75	0.00079	0.00012
1.25	0.0015	0.00017
1.75	0.0017	0.00028
2.25	0.0017	0.00047

Table 4. Adsorption equilibrium isotherms of Methylene Blue on clinoptilolite and on Amberlite XAD-4 (T= 20°C)

Clinoptilolite	Amberlite XAD-4
Langmuir Model	
K_A= 0.16 l/mg	K_A = 4.5 l/mg
q_m = 43.2 mg/g sorbent	q_m = 8.1 mg/g sorbent
(r^2 = 0.98)	(r^2 = 0.99)
Freundlich Model	
K_f = 7.24	K_f = 6.30
n = 0.59	n = 0.14
(r^2 = 0.92)	(r^2 = 0.96)

the removal of Methylene Blue. Similar results were obtained in our recent work (17) for the adsorption of Basic Yellow 28. The surface area of clinoptilolite evaluated by nitrogen adsorption is lower than the corresponding surface area of Amberlite XAD-4 (Table 2). However, clinoptilolite (a natural zeolite) is expected to have micropores beyond the limits of nitrogen adsorption analysis. Such micropore area is expected to contribute significantly to the adsorption rate and also to the adsorption capacity. Differences in hydrophylic properties and the surface acidities of the adsorbents also cause differences in adsorption rate and equilibrium parameters.

Adsorption rates of Methylene Blue on both adsorbents were also evaluated using the diffusion models (Models C and D) proposed in this work. In order to use these models, experimental zeroth moment values were evaluated by the numerical integration of equation (7) using the concentration decay data obtained with clinoptilolite and Amberlite XAD-4. These experimental zeroth moment values were then used for the evaluation of the effective diffusion coefficient of Methylene Blue in Model C (using equation (9)) and in Model D (using equation (11)). In the case of Model D, the observed adsorption equilibrium parameter K should be known in order to estimate the value of D_A from equation (11). K values are evaluated from equations (12) and (13) using the results reported in Table 4, for the Freundlich and the Langmuir adsorption isotherm models and the results are summarized in Tables 5 and 6, for Amberlite XAD-4 and clinoptilolite, respectively. The values of the effective diffusion coefficients are then evaluated for Amberlite XAD-4 and for clinoptilolite using equations (9) and (11) (Models C and D) and the results are also reported in Tables 5 and 6. As seen in Table 5, effective diffusion coefficients evaluated from Model C are almost independent of amount of adsorbate charged to the adsorber and independent of adsorbate concentration C_e. This is the major advantage of Model C over the other models. The average values of D_A evaluated from this model are 5.1×10^{-10} cm^2/s and 1.2×10^{-10} cm^2/s, for Amberlite XAD-4 and for clinoptilolite, respectively. The diffusivity values estimated from this model are based on the pseudohomogeneous particle

Table 5. Effective diffusion coefficients of Methylene Blue in Amberlite XAD-4 from Models C and D ($T = 20°C$)

				Model D			
			Model C	Langmuir model (equation (12))		Freundlich model (equation (11))	
w_s (g/l)	μ_o (s)	C_e (mg/l)	D_A (cm^2/s)	K (l/g)	D_A (cm^2/s)	K (l/g)	D_A (cm^2/s)
0.50	61800	10.0	$4.8\ 10^{-10}$	$1.7\ 10^{-2}$	$0.5\ 10^{-8}$	0.12	$3.0\ 10^{-8}$
0.75	58400	6.7	$5.0\ 10^{-10}$	$3.8\ 10^{-2}$	$1.1\ 10^{-8}$	0.17	$4.3\ 10^{-8}$
1.25	52800	3.8	$5.4\ 10^{-10}$	$11.1\ 10^{-2}$	$3.1\ 10^{-8}$	0.27	$6.3\ 10^{-8}$
1.50	54900	1.9	$5.3\ 10^{-10}$	$39.9\ 10^{-2}$	$7.5\ 10^{-8}$	0.51	$8.7\ 10^{-8}$

assumption. More realistically, effective pore diffusion coefficient may be estimated from $D_A^* = D_A\,\varepsilon_A$. The values of D_A^* are then become 2.7×10^{-10} cm^2/s and 0.64×10^{-10} cm^2/s for diffusion of Methylene Blue in Amberlite XAD-4 and in clinoptilolite, respectively.

In the case of Model D, effective diffusion coefficients were found to be highly concentration dependent (Tables 5 and 6) for both Langmuir and Freundlich adsorption isotherms. This concentration dependence is more significant for Amberlite XAD-4. The values of the effective diffusivities estimated from this model are about two orders of magnitude higher than the corresponding values estimated from Model C. The concentration dependence of the effective pore diffusion coefficient values evaluated from Model D indicated a strong interaction of the diffusing molecules

Table 6. Effective diffusion coefficients of Methylene Blue in clinoptilolite from Models C and D (T=20°C).

				Model D			
			Model C	Langmuir model (equation (12))		Freundlich model (equation (11))	
w_s (g/l)	μ_o (s)	C_e (mg/1)	D_A (cm^2/s)	K (l/g)	D_A (cm^2/s)	K (l/g)	D_A (cm^2/s)
0.28	33000	6.9	$1.1\ 10^{-10}$	1.6	$9.5\ 10^{-8}$	1.9	$1.1\ 10^{-7}$
0.39	22600	4.3	$1.6\ 10^{-10}$	2.4	$15.6\ 10^{-8}$	2.3	$1.5\ 10^{-7}$
0.69	29200	1.4	$1.3\ 10^{-10}$	4.6	$10.6\ 10^{-8}$	3.8	$1.0\ 10^{-7}$
1.14	33400	0.2	$1.1\ 10^{-10}$	6.5	$6.5\ 10^{-8}$	8.3	$0.7\ 10^{-7}$

with the pore surfaces. As reported in Table 5, the value of D_A significantly decreased with an increase in C_e, in Amberlite XAD-4. In Model D, adsorption and effective pore diffusion coefficients were considered as seperate terms. It is a two parameter and a more realistic but a more complex model than Model C. However, the concentration dependence of the effective diffusion coefficients evaluated from Model D limits its application. These results showed that Model C is a better representation for this system for applications in a large range of Methylene Blue concentrations. Another advantage of Model C is that it is a simpler model containing a single parameter.

Tortuosity factors of the adsorbents were then estimated from equation (14), using the diffusivity values obtained from Model D.

$$D_A = D_M(\varepsilon_A/\tau) \tag{14}$$

The molecular diffusion coefficient of Methylene Blue (D_M) in the solution was estimated from the Wilke and Chang model (26) as 3.6×10^{-6} cm^2/s at 20°C. The tortuosity factor evaluated for Amberlite XAD-4 by this procedure was found to be very high and it increased significantly with an increase in adsorbate concentration C_e (Table 7). This is an indication of a strong interaction of diffusing molecules with the pore surfaces. Methylene Blue is expected to adsorb strongly on the pore surfaces following a dissociative adsorption process. As a result, some pores are expected to be closed or blocked by the adsorbed molecules, which causes high tortuosity factors and also an increase in τ with an increase in C_e. The tortuosity factor evaluated for clinoptilolite was also quite high (Table 7), but it did not show an increasing trend with an increase in adsorbate concentration. This result indicated that the interaction of the adsorbate molecules with the pore surfaces of clinoptilolite is also quite high, but further closure of pores by the dissociation of Methylene Blue molecules at higher concencentrations is probably less significant than Amberlite XAD-4.

Table 7. Tortuosity factors (τ) evaluated at $T = 20$°C

Amberlite XAD-4			Clinoptilolite		
C_e (mg/l)	τ (Langmuir)	τ (Freundlich)	C_e (mg/l)	τ (Langmuir)	τ (Freundlich)
10.0	370	62	6.9	20	17
6.7	170	44	4.3	12	13
3.8	60	29	1.4	18	19
1.9	25	21	0.2	29	27

Temperature and pH Effects

To investigate the effect of temperature on the adsorption rate and equilibrium of Methylene Blue, a set of experiments were carried out in a temperature range between 20°C and 50°C. Typical results obtained using 0.25 g/l Amberlite XAD-4 and 0.39 g/l clinoptilolite charged to the adsorber are shown in Figs. 7 and 8, respecively. As shown in Figure 7, adsorption capacity showed a significant increase with an increase in temperature for Amberlite XAD-4. These results proved that, adsorption of Methylene Blue on Amberlite XAD-4 is not a simple physical adsorption process. Chemisorption and probably dissociative adsorption of Methylene Blue may explain this behavior. As shown in Fig. 8, a similar trend was observed in adsorption of Methylene Blue on clinoptilolite. However, the effect of temperature on the adsorption capacity is less for clinoptilolite than Amberlite XAD-4.

Adsorption equilibrium parameters of Langmuir adsorption isotherm evaluated from the adsorption equilibrium data obtained at different temperatures on Amberlite XAD-4 are given in Table 8. Increase in q_m value with an increase in temperature is an indication of increased availability of adsorption sites of Amberlite XAD-4 due to the higher penetration of Methylene Blue into the pores, at higher temperatures. A similar result was reported in our earlier study for the adsorption of ethanol on Amberlyst 15 (20). The

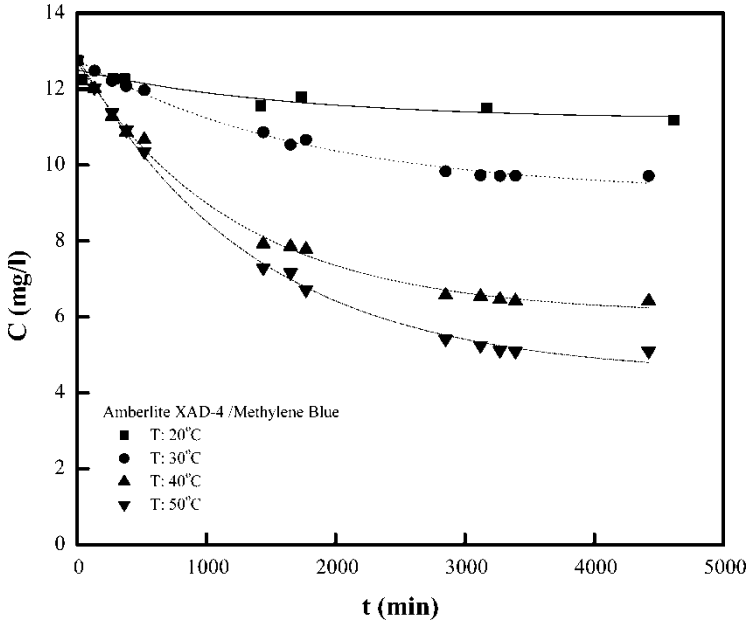

Figure 7. Temperature effects on Methylene Blue/Amberlite XAD-4 adsorption system ($w_s = 0.25$ g/l).

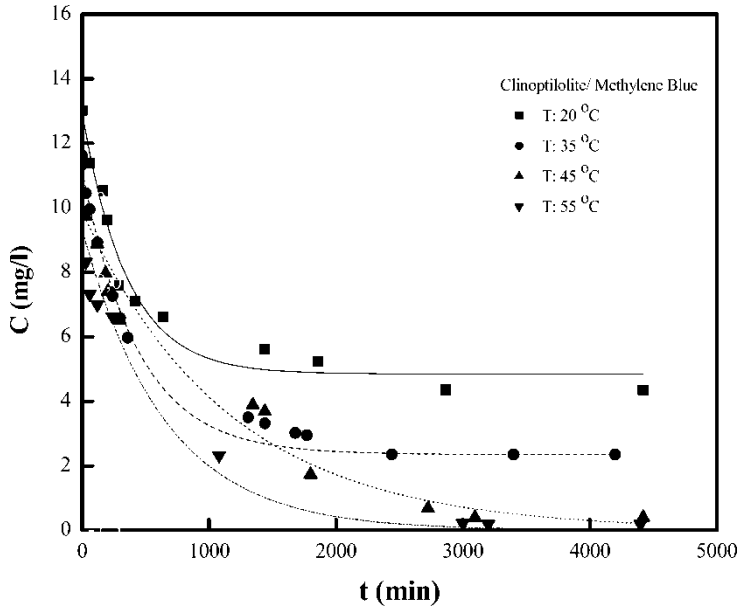

Figure 8. Temperature effects on Methylene Blue/clinoptilolite adsorption system ($w_s = 0.39\,g/l$).

effective diffusion coefficients of Methylene Blue evaluated at three different temperatures (20°C, 30°C, and 40°C) for both Models C and D are summarized in Table 9. Results reported in this table indicated that effective particle pseudohomogeneous diffusion coeffecient evaluated from Model C showed a decreasing trend with an increase in temperature. For instance, with a w_s value of 1.0 g/l, the effective diffusivity values evaluated from Model C decreased from 5.1×10^{-10} cm^2/s to 3.4×10^{-10} cm^2/s with an increase in temperature from 20 °C to 40 °C. The diffusivity of this model reflects the combined effect of diffusion and adsorption within the adsorbent. Higher dissociative adsorption of Methylene Blue might be a reason for this decrease of effective diffusivity with an increase in

Table 8. Adsorption equilibrium parameters of Methylene Blue on Amberlite XAD-4, at different temperatures. (Langmuir isotherm)

T (°C)	20	30	40
K_A (l/mg)	4.5	3.3	4.8
q_m (mg/g)	8.1	14.2	18.8
$K_A\,q_m$ (l/g)	36.5	46.9	90.2

Table 9. Effective diffusion coefficients of Methylene Blue in Amberlite XAD-4 at different temperatures, for Models C and D

			Model C	Model D with Langmuir isotherm	
w_s (g/l)	μ_o (s)	C_e (mg/l)	D_A (cm^2/s)	K (l/g)	D_A (cm^2/s)
T: 20°C					
1.00	58400	5.6	$5.1\ 10^{-10}$	$5.3\ 10^{-2}$	$1.5\ 10^{-8}$
T: 30°C					
0.5	75100	9.7	$3.9\ 10^{-10}$	$4.3\ 10^{-2}$	$1.0\ 10^{-8}$
0.75	62700	6.4	$4.7\ 10^{-10}$	$9.5\ 10^{-2}$	$2.3\ 10^{-8}$
1.00	66900	5.1	$4.4\ 10^{-10}$	$14.8\ 10^{-2}$	$3.2\ 10^{-8}$
1.25	59200	3.4	$4.9\ 10^{-10}$	$31.4\ 10^{-2}$	$6.3\ 10^{-8}$
1.50	63000	1.5	$4.7\ 10^{-10}$	$132.0\ 10^{-2}$	$11.6\ 10^{-8}$
T: 40°C					
1.00	86300	1.7	$3.4\ 10^{-10}$	$107.5\ 10^{-2}$	$9.9\ 10^{-8}$

temperature. However, in Model D diffusion and the adsorption were considered as separate terms. For Model D, the effective diffusivity values increased with an increase in temperature (Table 9). For a system with a large molecular size of adsorbate (like Methylene Blue), interaction of diffusing molecules with the pore walls is inevitable. In such systems, surface diffusion may also become important. As shown in Table 9, the effective diffusivity values evaluated at 30°C were also found to be highly concentration dependent for Model D, while the diffusion coefficients obtained for Model C were almost constant. These results are in agreement with the results obtained at 20°C (Table 5) and supports our conclusion that Model C is a better representation of the system for practical applications.

Apparent first order rate constant values of Methylene Blue on Amberlite XAD-4 and on clinoptilolite are evaluated at different temperatures from the slopes of the lines given in Figs. 9 and 10 and the results are reported in Table 10. As it was discussed before, for this model the adsorption rate constant values were highly dependent on the adsorbate concentration and the amount of adsorbent charged to the adsorber. This is the major limitation of the pseudo-first order adsorption rate model. In the case of pseudo-second order adsorption rate model (Model B), the agreement of the experimental data with the predictions of equation (4) were rather poor at all temperatures and no further attempt was made for the analysis of the data to evaluate the second order adsorption rate constants.

In some experiments, pH of the solution was measured as a function of time. Results showed that pH remained almost constant between 6.5

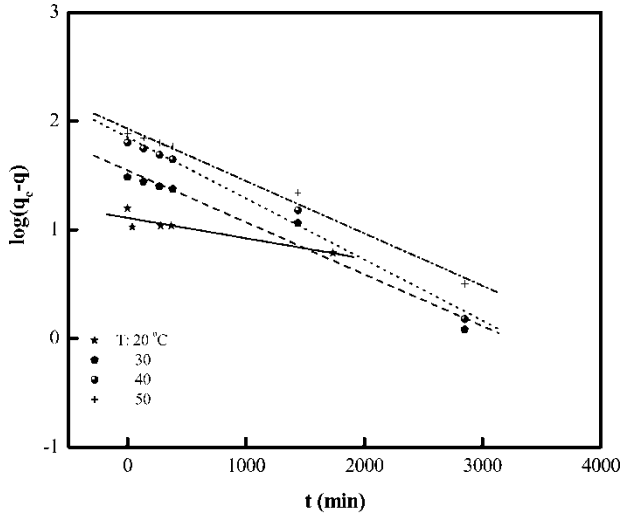

Figure 9. Typical Lagergren plots for adsorption of Methylene Blue on Amberlite XAD-4 at various temperatures ($w_s = 0.25$ g/l).

and 7 throughout an adsorption run. In order to investigate the effect of pH on the adsorption rate, a set of experiments were carried out at different pH values with both clinoptilolite and Amberlite XAD-4, at 20°C. Results reported in Fig. 11 showed that, the pH of the solution

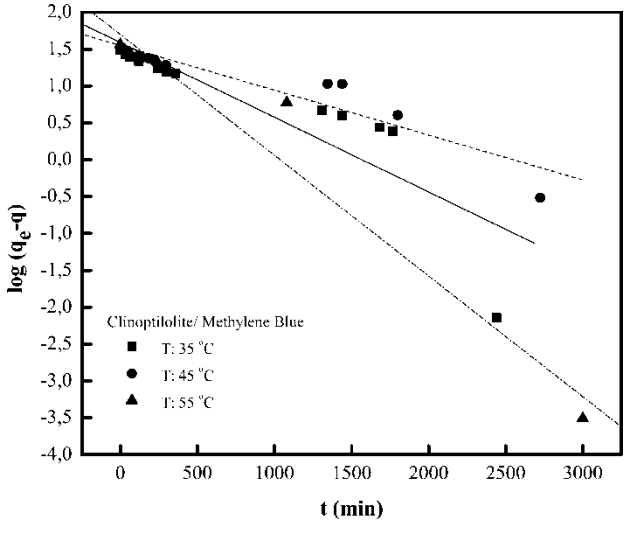

Figure 10. Typical Lagergren plots for adsorption of Methylene Blue on clinoptilolite at various temperatures ($w_s = 0.39$ g/l).

Table 10. Adsorption rate constants of Methylene Blue from Model A (pseudo-first order adsorption rate) at different temperatures

T°C	k_1 (min^{-1}) Amberlite XAD-4 ($w_s = 0.25$ g/l)	k_1 (min^{-1}) Clinoptilolite ($w_s = 0.39$ g/l)
20	0.00039	0.0015
30	0.0011	—
35	—	0.0013
40	0.0013	—
45	—	0.0014
50	0.0011	—
55	—	0.0016

had a significant effect on the adsorption rate and equilibrium, for Amberlite XAD-4. Adsorption capacity increased from 6 mg/g to about 18 mg/g by decreasing the pH from 10 to 3. The effect of pH was found to be less significant for clinoptilolite in the pH range between 8 and 3 (Fig. 12). However, at a pH value of 10 a significant decrease was observed in the adsorption capacity of Methylene Blue on clinoptilolite. The adsorption capacity values were found to be about 16 mg/g and

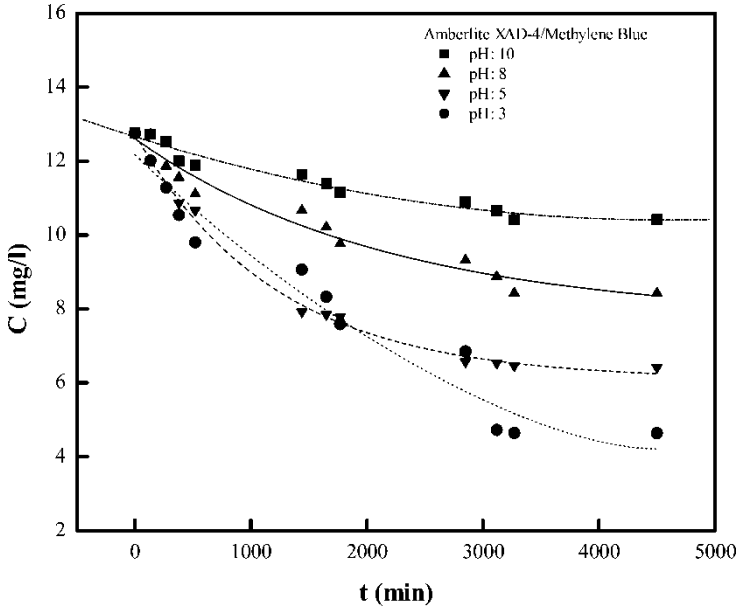

Figure 11. pH effect for Methylene Blue adsorption on Amberlite XAD-4 ($w_s = 0.50$ g/l; $T = 20$°C).

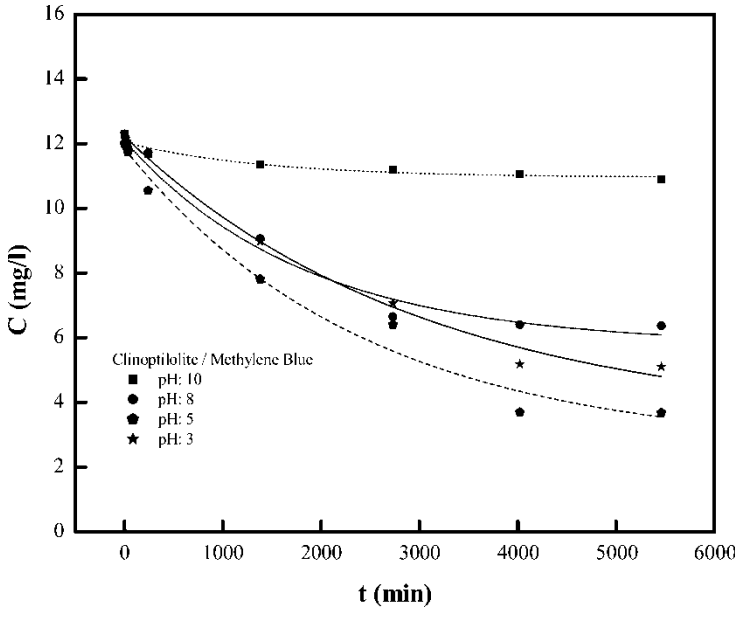

Figure 12. pH effect for Methylene Blue adsorption on clinoptilolite($w_s = 0.50$ g/l; $T = 20°C$).

24 mg/g (for $w_s = 0.50$ g/l at 20°C) for this adsorbent, at pH values of 8 and 3, respectively.

CONCLUSIONS

Adsorption rate and the equilibrium studies carried out with Methylene Blue showed that clinoptilolite was a better sorbent than Amberlite XAD-4 at 20°C and at a pH of 7. Among the two adsorption rate models which do not consider pore diffusion effects, pseudo-first order rate model (Model A) gave better agreement with the experimental data than the pseudo-second order model. However, the major limitation of this model is the dependence of the observed adsorption rate constant to the amount of adsorbent and to the concentration of the adsorbate. Among the other two models (Models C and D) which consider pore diffusion resistance, Model C is a single parameter model and the effective diffusivity evaluated from this model was found to be not dependent on the adsorbate concenration. This is the major advantage of this model over all three of the other models. It is concluded that Model C is the best model for the estimation of the rate of adsorption of this dye on both adsorbents studied. Although Model D (in which

adsorption and pore diffusion terms were both considered separately) is a more realistic model, diffusion coefficient of this model was found to be highly dependent on the concentration of the adsorbate. This is to a great extent due to the strong interaction of the adsorbate with the pore walls of the adsorbent during penetration into the particle. Results also showed that adsorbate molecules were strongly adsorbed on the pore surfaces, probably following a dissociative chemisorption step and this caused plugging of some of the pores. High values of the tortuosity factors evaluated for both adsorbents and the increase of the tortuosity with an increase in adsorbate concentration, supported this conclusion. It was also shown that, for Amberlite XAD-4 adsorption capacity was increased with an increase in temperature, probably due to the increased availibility of the active sites because of the higher penetration of the adsorbate molecules into the pores, at higher temperatures. The pH of the solution was almost constant during an adsorption run for both adsorbents. However, a significant increase in adsorption capacity was observed with a decrease in pH from 10 to 3, especially for Amberlite XAD-4. Another important conclusion of this work is that effective diffusion coefficient of an adsorbate in a porous adsorbent can be easily evaluated by the moment analysis of the concentration decay curves obtained in a batch adsorber.

NOMENCLATURE

C	liquid phase concentration of adsorbate in the batch adsorber (mg/l)
C_A	concentration of adsorbate in the pores of the adsorbent (mg/l)
C_o	initial liquid-phase concentration of adsorbate (mg/l)
C_e	equilibrium liquid-phase concentration (mg/l)
D_A	effective diffusion coefficient (cm^2/s)
D_A^*	effective pore diffusion coefficient, defined as $D_A^* = D_A\ \varepsilon_A$ (cm^2/s)
K	apparent adsorption equilibrium constant defined in equations (12) and (13) (l/g)
K_A	adsorption equilibrium constant in Langmuir isotherm (l/mg)
k_1	rate constant of pseudo-first order adsorption (s^{-1})
k_1^*	adsorption rate constant (Equation (1)) ($l/mg \cdot s$)
k_{-1}^*	desorption rate constant (Equation (1)) (s^{-1})
k_2	rate constant of pseudo-second-order adsorption. ($g/mg \cdot s$)
n	Freundlich exponent
q_e	adsorbed concentration of adsorbate at equilibrium (mg/g)
q_m	maximum adsorbed concentration per unit mass of adsorbent (mg/g)

R	radial coordinate in the spherical adsorbent particles
R_o	average particle radius (cm)
T	temperature (°C)
w_s	amount of adsorbent (g/l)
μ_o	zeroth moment defined by equation (7) (s)
ρ_p	apparent density of the adsorbent (g/cm^3)
ε_A	porosity of the adsorbent

ACKNOWLEDGEMENTS

This work was funded by Research Fund AFP97-111-003-03 and DPT98K123190 of Zonguldak Karaelmas University, Zonguldak, Turkey.

REFERENCES

1. McKay, G. (1982) Adsorption of dystuffs from aqueous solutions with activated carbon I: equilibrium and batch contact-time studies. *J. Chem. Tech. Biotechnol*, 32: 759–772.
2. McKay, G. (1982) Adsorption of dystuffs from aqueous solutions with activated carbon II: column studies and simplified design models. *J. Chem. Tech. Biotechnol*, 32: 773–780.
3. McKay, G., Otterburn, M., and Saga, J.A. (1985) Fuller's earth and fired clay as adsorbents for dyestuffs. *Water Air and Soil Pollution*, 24: 307–322.
4. McKay, G., Ramprasad, G., and Mowli, P.P. (1986) Desorption and regeneration of dye colours from low-cost materials. *Water Air and Soil Pollution*, 29: 273–283.
5. McKay, G., Ramprasad, G., and Mowli, P.P. (1987a) *Water Research*, 21: 375–377.
6. McKay, G., Geundi, M.E., and Nassar, M.M. (1987b) Equilibrium studies during the removal of dyestuffs from aqueous solutions using bagasse pith. *Water Research*, 21: 1513–1520.
7. De, D.K., Kanungo, J.L.D., and Chakravarti, S.K. (1974a) *Indian Journal of Chemistry*, 12: 165–166.
8. De, D.K., Kanungo, J.L.D., and Chakravarti, S.K. (1974b) *Indian Journal of Chemistry*, 12: 1187–1189.
9. Narine, D.R. and Guy, R.D. (1981) *Clays Clay Miner*, 29: 205–212.
10. Perineau, F., Molinier, J., and Gaset, A. (1982) Adsorption of ionic dyes on charred plant material. *J. Chem. Tech. Biotechnol*, 32: 749–758.
11. Asfour, H.M., Nassar, M.M., Fadali, O.A., and El-Geundi, M.S. (1985) Colour removal from textile effluents using hardwood sawdust as an absorbent. *J. Chem. Tech. Biotechnol*, 35: 28–35.
12. Khokhlova, T.D., Nikitin, Y.S., Detistova, A.L., and Garkavenko, L.G. (1991) Study of the chemistry of the surfaces of modified silicas with the aid of the adsorption of dyes. *Zhurnal Fizicheskoi Khimii*, 65: 2705–2708.
13. Meyer, V., Carlsson, F.H.H., and Oellermann, R.A. (1992) Decolourization of textile effluents using a low cost natural adsorbent material. *Water. Sci. Technol*, 126: 1205–1211.

14. Khare, S.K., Panday, K.K., Srivastava, R.M., and Singh, V.N. (1987) Removal of victoria blue from aqueous solution by fly ash. *J. Chem. Tech. Biotechnol*, 38: 99–104.
15. Gupta, G.S., Prasad, G., and Singh, V.N. (1990) Removal of chrome dye from aqueous solutions by mixed adsorbents: fly ash and coal. *Water Research*, 24: 45–50.
16. Lee, C.K., Low, K.S., and Chow, S.W. (1996) Chrome sludge as an adsorbent for colour removal. *Environmental Technology*, 17: 1023–1028.
17. Yener, J., Kopac, T., Dogu, G., and Dogu, T. (2006) Adsorption of Basic Yellow 28 from aqueous solutions with clinoptilolite and Amberlite. *J. Coll. Interf. Sci*, 294: 255–264.
18. Wang, Y.X. and Yu, J. (1998) Adsorption and degradation of synthetic dyes on the mycelium of trametes versicolor. *Water Sci. Technol*, 38: 233–238.
19. Rubin, E., Rodrigea, P., Herrero, R., Cremades, J., Barbara, I., and Vicente, M. (2005) Removal of Methylene Blue rom aqueous solutions using as biosorbent Sargassum Muticum: an invasive macroalga in Europe. *J. Chem. Tech. Biotechnol*, 80: 291–298.
20. Doğu, T., Aydın, E., Boz, N., Murtezaoğlu, K., and Doğu, G. (2003) Diffusion resistances and contribution of surface diffusion in TAME and TAEE production using amberlyst-15. *International Journal of Chemical Reactor Engineering*, 1 (A6): 1–10. http://www.bepress.com/ijcre/vol1/A6/.
21. Kopac, T., Dogu, G., and Dogu, T. (1996) Single pellet reactor for the dynamic analysis of gas-solid reactions. *Chem. Eng. Sci*, 51: 2201–2209.
22. Oktar, N., Murtezaoglu, K., Dogu, T., and Dogu, G. (1999) Dynamic analysis of adsorption equilibrium and rate parameters of reactants and products in MTBE, ETBE and TAME production. *Can. J. Chem. Eng*, 77: 406–412.
23. Furusawa, T. and Suzuki, M. (1975) Moment analysis of concentration decay in a batch adsorption vessel. *J. Chem. Eng. Japan*, 8: 119–122.
24. Dogu, G. and Smith, J.M. (1976) Rate parameters from dynamic experiments with single catalyst pellets. *Chem. Eng. Sci.*, 31: 123–128.
25. MERCK Catalog, Technical Data Sheet, KgaA, D-6421 Darmstadt. 2005 http://chemdat.merck.de/mda/int_en/index.html.
26. Liu, J.G., Luo, G.S., Pan, S., and Wang, J.D. (2004) Diffusion coefficients of carboxylic acids in mixed solvents of water and 1-butanol. *Chem. Eng. and Processing*, 43: 43–47.